

Probing the Hole Dispersion Curves of a Quantum Well Using Resonant Magnetotunneling Spectroscopy

R. K. Hayden,⁽¹⁾ D. K. Maude,⁽¹⁾ L. Eaves,⁽¹⁾ E. C. Valadares,⁽¹⁾ M. Henini,⁽¹⁾ F. W. Sheard,⁽¹⁾ O. H. Hughes,⁽¹⁾ J. C. Portal,⁽²⁾ and L. Cury⁽²⁾

⁽¹⁾Department of Physics, University of Nottingham, Nottingham, NG7 2RD, United Kingdom

⁽²⁾Laboratoire de Physiques des Solides, Institut National des Science Appliquées, F31077 Toulouse, France and Service National des Champs Intenses, Centre National de la Recherche Scientifique, F38042 Grenoble, France
(Received 12 December 1990)

We describe a novel magnetotunneling spectroscopy technique for probing the complicated dispersion curves of hole states in the quantum well of p -type double-barrier resonant-tunneling structures. Strong mixing between light- and heavy-hole states is observed. Some of the states clearly exhibit a negative hole effective mass for motion in the plane of the quantum well.

PACS numbers: 73.20.Dx, 73.40.Gk

In bulk semiconductors, the low-energy dispersion curves of the light- and heavy-hole valence bands are parabolic.^{1,2} However, when a quantizing magnetic field ($\mathbf{B}\parallel z$) is applied to a bulk semiconductor, the quantized hole energies, or Landau levels, are complicated functions of wave-vector component k_z .¹⁻³ A confining quantum-well potential also produces complicated hole dispersion curves as a function of the in-plane wave-vector component k_{\parallel} , even at zero magnetic field.⁴⁻⁷ In both cases the complexity is due to the admixing of light-hole (LH) and heavy-hole (HH) states due to the spin-orbit interaction. There have been relatively few experimental investigations of the hole dispersion curves in quantum wells because spectroscopic techniques tend to average over k space.

In this Letter we describe a novel experimental technique, namely, resonant magnetotunneling spectroscopy, for probing directly the resonant-magnetotunneling spectroscopy, for probing directly the dispersion curves of holes in a quantum well. We study the effect of a large magnetic field applied parallel to the plane of the barriers on the current-voltage characteristics, $I(V)$, of p -type double-barrier resonant-tunneling structures. Tunneling holes acquire a large k_{\parallel} due to the magnetic field. The resulting shift in the voltage positions of the resonant peaks in $I(V)$ reveals the light-hole-heavy-hole admixing and shows clearly that some states correspond to a negative hole effective mass for motion in the plane of the quantum well; i.e., *increased* hole momentum in the plane of the barriers corresponds to *decreased* kinetic energy. Some evidence of light-hole-heavy-hole mixing has been reported in a previous study of resonant tunneling in the p -type GaAs/AlAs system.⁸ Recent calculations⁹ of hole states in resonant-tunneling devices have shown that the complicated nature of the valence band strongly influences $I(V)$.

Here we consider two devices grown by molecular-beam epitaxy. The composition and valence-band-bending diagram of device 1 at an applied voltage V are

shown schematically in Fig. 1. At low temperatures a degenerate two-dimensional hole gas (2DHG) forms in an accumulation layer in the undoped region adjacent to the emitter barrier. The quasibound states in the quantum well are given their conventional notation at $k_{\parallel}=0$, where there is no mixing between light and heavy holes.

Device 1 comprises the following layers in order of growth on a GaAs substrate: 3- μm -thick GaAs lower contact layer, Be doped to $p=2\times 10^{18}\text{ cm}^{-3}$; 100-nm GaAs, $p=1\times 10^{18}\text{ cm}^{-3}$; 100-nm GaAs, $p=5\times 10^{17}\text{ cm}^{-3}$; 5.1-nm undoped GaAs spacer layer; 5.1-nm undoped AlAs barrier; 4.2-nm undoped GaAs quantum well; 5.1-nm undoped AlAs barrier; 5.1-nm undoped GaAs spacer layer; 100-nm GaAs, $p=5\times 10^{17}\text{ cm}^{-3}$;

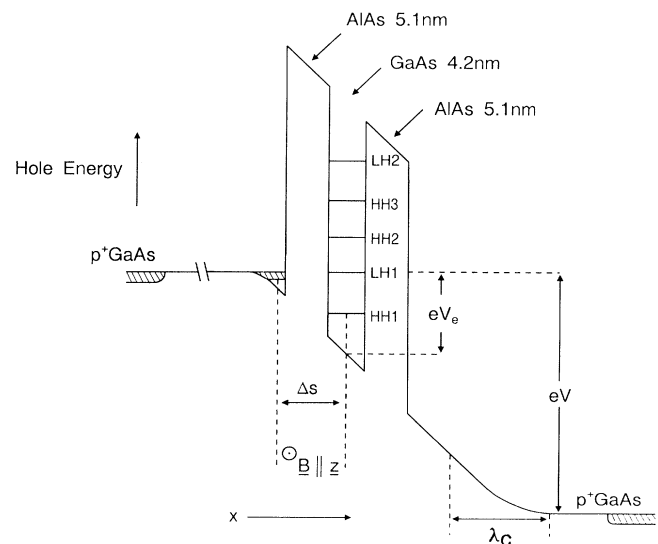


FIG. 1. Schematic diagram of the valence-band profile of p -type resonant-tunneling device 1 under an applied voltage V . Note that a two-dimensional hole gas forms in the accumulation layer adjacent to the emitter barrier. Device 2 is identical except that the quantum well is 6.8 nm wide.

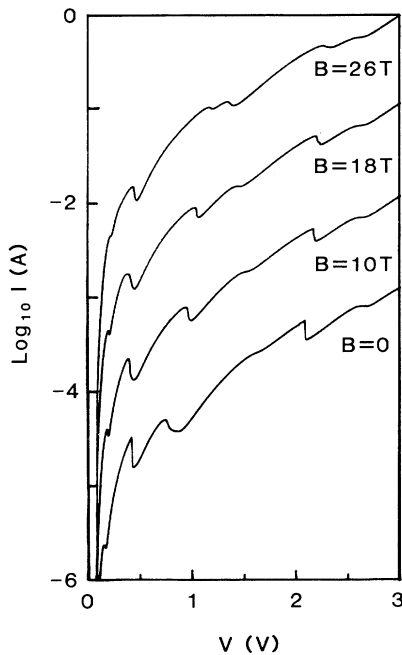


FIG. 2. Logarithmic plots of the $I(V)$ characteristics of device 1 (quantum-well width 4.2 nm) at various in-plane magnetic-field values, $T=4.2$ K. The logarithmic vertical axis gives the current for $B=0$. For clarity, the curves for 10, 18, and 26 T are displaced upwards by 1, 2, and 3 orders of magnitude, respectively.

100-nm GaAs, $p=1 \times 10^{18} \text{ cm}^{-3}$; GaAs top contact layer, $0.6 \mu\text{m}$, $p=2 \times 10^{18} \text{ cm}^{-3}$. Device 2 differs only in the quantum-well width (6.8 nm). Both devices were processed into 100- μm -diam mesas.

Figure 2 shows the $I(V)$ characteristics for device 1 at 4.2 K. Six peaks are observed in $I(V)$, corresponding to resonant tunneling from the emitter 2DHG into the various quasibound states of the quantum well. Peak-to-valley current ratios of up to 3:1 are observed. The figure shows the variation of $I(V)$ with transverse magnetic field (\mathbf{B} perpendicular to the current flow \mathbf{J}) up to 26 T. Figure 3(a) plots the voltage positions of the peaks V_p as a function of B . The different resonances have quite different magnetic-field dependences. The HH1 and LH1 resonances shift very little, whereas the HH2 and HH3 resonances shift appreciably in opposite senses and “anticross” at $B \approx 26$ T. This behavior differs markedly from the effect of a transverse magnetic field on the $I(V)$ characteristics of n -type resonant-tunneling devices: For electrons the resonant peaks shift to higher bias,¹⁰ quadratically with B , in accordance with the effective-mass approximation.¹¹⁻¹³ The shape of the $V(B)$ curves of Fig. 3(a) shows a remarkable resemblance to the $\epsilon(k_{\parallel})$ dispersion curves of hole states in a quantum well. Such a curve is shown in Fig. 3(b) for a 4.2-nm-wide isolated AlAs/GaAs/AlAs quantum well in zero electric and magnetic fields, calculated using a

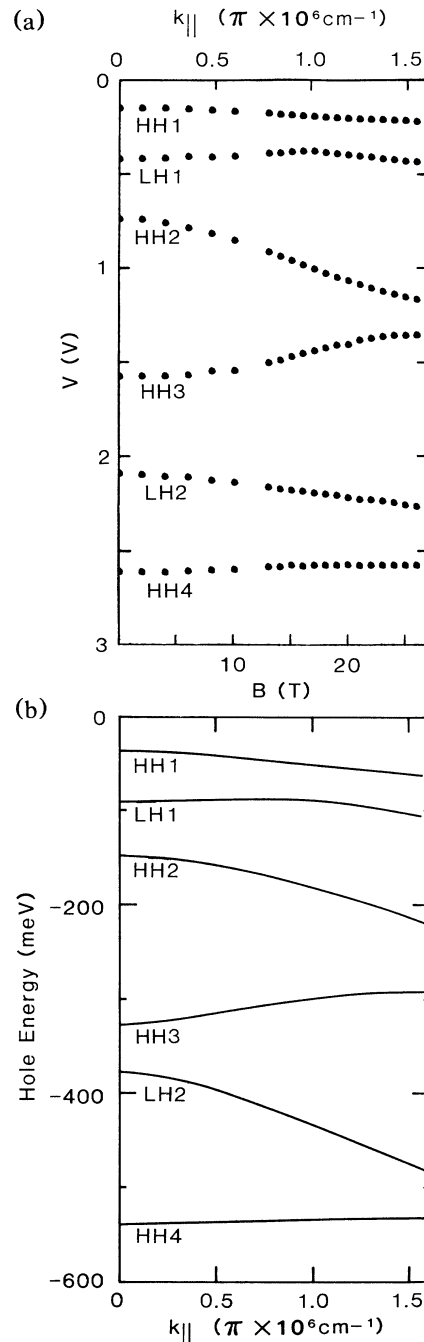


FIG. 3. (a) Variation in the voltage position of the peaks in $I(V)$ as a function of in-plane magnetic field for device 1. The value of k_{\parallel} is obtained from Eq. (1) in the text. (b) Calculated hole dispersion curves for an isolated AlAs/GaAs/AlAs quantum well 4.2 nm wide in zero electric and magnetic fields.

four-component envelope-function formalism.⁶ The dispersion curves for an isolated hole quantum well do not differ appreciably from those for a well with finite barriers if the two barriers are sufficiently wide,⁹ as is the case here. A comparison between Figs. 3(a) and 3(b)

reveals the qualitative similarity between the calculated $\varepsilon(k_{\parallel})$ curves for the HH1, LH1, HH2, and HH3 states and the corresponding $V(B)$ curves. The only major difference is the larger dispersion obtained from theory for the LH2 resonance.⁶

The essential principle underlying our experiments is that the applied voltage tunes the energy of the occupied hole states in the emitter 2DHG to that of the quantum-well states, while the magnetic field allows us to probe different values of k_{\parallel} . The $V(B)$ plots therefore map out the $\varepsilon(k_{\parallel})$ dispersion curves of the hole states in the quantum well.

Quantum mechanically, the effect of a magnetic field ($\mathbf{B} \parallel z$) on the motion of a particle (electron or hole) of charge q is found by replacing the canonical momentum operator p_y by $p_y - qBx$, using the Landau gauge $\mathbf{A} = (0, Bx, 0)$. The extra term, $-qBx$, gives rise to a magnetic contribution to the effective potential governing motion along the x direction, normal to the barrier interfaces.¹⁴ However, it does not affect the plane-wave nature of the states in the k_y and k_z directions, so that $p_y = \hbar k_y$ is a constant of motion. For the localized quasibound states in the emitter accumulation layer and quantum well, the magnetic field can be treated as a perturbation. This is equivalent to replacing $\hbar k_y$ by $\hbar k_y - qB\langle x \rangle$, where $\langle x \rangle$ is the position coordinate averaged over the localized state. Thus, comparing the in-plane dispersion curves of the emitter accumulation layer and quantum-well states, we see that there is a relative displacement along the k_y axis by an amount

$$k_{\parallel} \equiv \Delta k_y = eB\Delta s / \hbar, \quad (1)$$

where Δs is the average separation between the bound states of the accumulation layer and quantum well. Taking the particles to be localized in the middle of the quantum well, we have $\Delta s = \lambda + b_1 + w/2$, where λ is the average standoff distance of the accumulation-layer charge from the barrier interface (which may be estimated from the Fang-Howard variational model¹⁵), b_1 is the emitter barrier width, and w is the quantum-well width. The occupied states below the Fermi level in the emitter accumulation layer are centered around $k_y = 0$ (Ref. 16) and $k_z = 0$. In the absence of scattering k_y , k_z , and energy are conserved in the tunneling transition.^{13,14,17} The available set of states in the quantum well are shifted in k_y by an amount given by Eq. (1).

For the case of resonantly tunneling conduction electrons, this change in k_y broadens the resonance in $I(V)$ and shifts it to higher voltages. The peak of the resonance corresponds to electrons with $k_y = 0$ and $-k_F \leq k_z \leq k_F$ in the emitter accumulation layer.¹¹⁻¹³ The shift is given by the simple quadratic $\varepsilon(k)$ dispersion curve of the conduction electrons and can be understood as follows: The magnetic field does no work on the electrons and, to maintain the resonance condition, any gain in kinetic energy corresponding to increased k_y must be

compensated by an additional applied voltage.

We now consider the more complicated case of holes and use Eq. (1) to determine the in-plane momentum k_{\parallel} acquired by a resonantly tunneling hole in a magnetic field B . These values of k_{\parallel} are plotted on the upper horizontal axis of Fig. 3(a) and 4, assuming $\lambda = 5$ nm for the hole accumulation layer.¹⁵ The large shift of the HH3 resonant peak to lower voltage with increasing B agrees qualitatively with theory and reveals the negative effective mass of these states. We also observe a much smaller negative-effective-mass behavior for the LH1 resonance over a range of k_{\parallel} from 0 to $\pi \times 10^6$ cm⁻¹, again in agreement with theory. Note also that the HH2 and HH3 curves are strongly dispersed in opposite senses, approaching each other at low B (low k_{\parallel}) and starting to repel each other at $B \approx 26$ T ($k_{\parallel} \approx 1.5\pi \times 10^6$ cm⁻¹). Such an anticrossing interaction is expected⁷ at this value of k_{\parallel} ($\approx \pi/w$) for a well width of 4.2 nm. Note from Fig. 2 that the strengths of these two resonances in $I(V)$ become comparable as the admixing increases.

The holes tunnel into a quantum-well state of energy eV_e , where V_e is the potential difference between the emitter and the center of the well (see Fig. 1). Neglecting the charge in the quantum well, we obtain the follow-

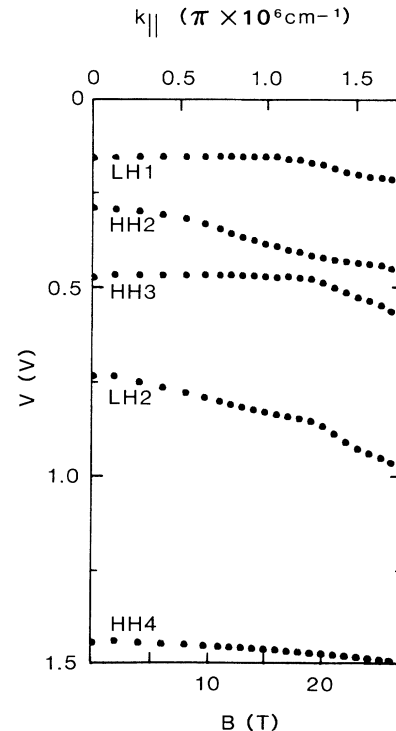


FIG. 4. Variation in the voltage position of the peaks in $I(V)$ as a function of in-plane magnetic field for device 2. The HH1 resonance is too weak to be observed in the $I(V)$ characteristics of this device, though a weak feature is observed in $C(V)$.

ing relation between V_e and the applied voltage V :

$$V/V_e = 1 + (w/2 + b_2 + u + \lambda_c) / (\lambda + b_1 + w/2),$$

where λ_c is the V -dependent collector screening length, b_2 is the collector barrier width, and u is the thickness of the undoped GaAs layer near the collector barrier. We estimate that this ratio takes the values $V/V_e = 2.9, 3.4, 4.3,$ and 5.0 for applied voltages $V = 0.5, 1.0, 2.0,$ and 3.0 V, respectively. Given the uncertainties in this estimate,¹⁸ these values are comparable with the scaling factor ($=5$) between the vertical axes of Figs. 3(a) and (b). They indicate that our method provides at least a qualitative measure of the energy dispersion of the hole states in the quantum well.

To further test the validity of Eq. (1) for hole tunneling, we have repeated the measurements for several devices with a variety of well and barrier widths. The $V(B)$ plot of the resonances for a well width of 6.8 nm (device 2) is shown in Fig. 4 and reveals the anticrossing of the HH2 and HH3 dispersion curves at a lower value of $k_{\parallel} \approx 1.2\pi \times 10^6 \text{ cm}^{-1}$, as expected for the wider well.

We have also investigated the anisotropy of the resonances when the magnetic field is rotated in the plane of the barriers. Only very small differences are observed for \mathbf{B} parallel to the [100] and [110] axes, indicating that anisotropy effects are relatively small for hole resonant tunneling in the GaAs/AlAs system.⁶ This indicates that the effect of the cubic symmetry term in the Luttinger Hamiltonian is small and partly justifies the use of Eq. (1) for holes. We have found no evidence in the $I(V)$ curves for spin splitting of the hole states due to applied magnetic and electric fields.⁷

In conclusion, we have investigated resonant tunneling of holes in double-barrier structures in the presence of a magnetic field applied parallel to the plane of the barriers. The resonances in $I(V)$ have a much more complicated dependence on B than is the case for electrons. A quantitative comparison of our experiments with theory requires a knowledge of the distribution of charge throughout the device. A detailed model of hole resonant tunneling in a transverse magnetic field should include the split-off band, especially for higher bound states. It should also describe the states in the emitter 2DHG, taking into account the finite spread of the in-plane wave vector, and should consider the effect of the large electric field ($> 10^7$ V/m) on the hole states in the quantum well. At fields $B > 20$ T, a nonperturbative approach is necessary since the magnetic length $(\hbar/eB)^{1/2}$ is comparable with the electrical confinement length w . However, despite the complexity of the system, we believe our measurements provide a new method of investigating the complicated in-plane dispersion curves and the negative-effective-mass behavior of hole states in quantum-well heterostructures.

This work is supported by the Science and Engineering Research Council, Centre National de la Recherche

Scientifique, and the European Community. We acknowledge invaluable discussions with R. Wessel, Professor M. Altarelli, Dr. M. L. Leadbeater, and Dr. G. A. Toombs.

¹J. M. Luttinger and W. Kohn, Phys. Rev. **97**, 869 (1955).

²J. M. Luttinger, Phys. Rev. **102**, 1030 (1956).

³J. C. Hensel and K. Suzuki, Phys. Rev. B **9**, 4219 (1974).

⁴D. A. Broido and L. J. Sham, Phys. Rev. B **31**, 888 (1985).

⁵A. Pinczuk, H. L. Stormer, A. C. Gossard, and W. Wiegmann, in *Proceedings of the Seventeenth International Conference on the Physics of Semiconductors*, edited by J. D. Chadi and W. A. Harrison (Springer, Berlin, 1985).

⁶L. C. Andreani, A. Pasquarello, and F. Bassani, Phys. Rev. B **36**, 5887 (1987). Such an approximation neglects the split-off valence bands and is only valid for the lower-energy bound states of the well. For GaAs, the spin-orbit splitting is $\Delta = 340$ meV. Neglecting the split-off bands may also change the order of the bound states at higher hole energy from that given in Figs. 3 and 4.

⁷G. Bastard, *Wave Mechanics Applied to Semiconductor Heterostructures* (Les Editions de Physique, Paris, 1988).

⁸E. E. Mendez, W. I. Wang, B. Ricco, and L. Esaki, Appl. Phys. Lett. **47**, 415 (1977).

⁹R. Wessel and M. Altarelli, Phys. Rev. B **39**, 12802 (1989).

¹⁰E. E. Mendez, L. Esaki, and W. I. Wang, Phys. Rev. B **33**, 2893 (1986).

¹¹L. Eaves, K. W. H. Stevens, and F. W. Sheard, in *The Physics and Fabrication of Microstructures and Microdevices*, edited by M. J. Kelly and C. Weisbuch, Springer Proceedings in Physics Vol. 13 (Springer, Berlin, 1986), p. 343.

¹²R. A. Davies, D. J. Newson, T. G. Powell, M. J. Kelly, and H. W. Myron, Semicond. Sci. Technol. **2**, 61 (1987).

¹³M. L. Leadbeater, L. Eaves, P. E. Simmonds, G. A. Toombs, F. W. Sheard, P. A. Claxton, G. Hill, and M. A. Pate, Solid-State Electron. **31**, 707 (1988).

¹⁴B. R. Snell, K. S. Chan, F. W. Sheard, L. Eaves, G. A. Toombs, D. K. Maude, J. C. Portal, S. J. Bass, P. Claxton, G. Hill, and M. A. Pate, Phys. Rev. Lett. **59**, 2806 (1987).

¹⁵F. F. Fang and W. E. Howard, Phys. Rev. Lett. **16**, 797 (1966); F. Stern and W. E. Howard, Phys. Rev. **163**, 816 (1967).

¹⁶This is equivalent to choosing the origin of coordinates such that $\langle x \rangle = 0$ for the bound state in the accumulation layer.

¹⁷Although the dwell times in the quantum well and accumulation layer are long enough for particles to scatter and thermalize [see M. L. Leadbeater *et al.*, J. Phys. Condens. Matter **1**, 10605 (1989)], the Landauer-Buttiker-Stevens traversal time across the barrier in our experiment is very short, $\approx 10^{-14}$ s, so that the tunneling transition itself can be regarded as ballistic (see Ref. 11).

¹⁸The estimates of V/V_e assume that the Be acceptors in the heavily doped regions have not diffused from their nominal positions and that there is a sharp interface between the depleted (fully ionized acceptors) and undepleted (neutral acceptors) parts of the collector. Hole space charge in the quantum well would increase the ratio V/V_e somewhat. The effect of the magnetic field on this ratio should be fairly weak as it shifts the resonance by a relatively small amount.